Available online at www.sciencedirect.com

ScienceDirect

Procedia Engineering 10 (2011) 1742–1747

Engineering Procedia

ICM11

Elasto-Plastic Response of Impacted Moderatly Thick Rectangular Plates with Different Boundary Conditions

Korosh Khorshidi[a*]

[a] *Department of Mechanical Engineering, Faculty of Engineering, Arak University, Arak, 38156-88349, Iran.*

Abstract

Many elements of structures are subject to dynamic loads during their operation. Knowing the structure's dynamic response parameters makes it possible to design the structure with account of design, strength and operational requirements. Impact of a sphere with a plane surface is a common phenomenon in nature. Rectangular plates subjected to external loads with different boundary conditions have undoubtedly been one of the key components in aerospace, civil, automotive, biomechanical, petrochemical, marine industries, nuclear, optical, electronic, mechanical, and shipbuilding industries. This paper introduces semi-analytically solution for the elasto-plastic analysis of the isotropic rectangular plates subjected to transverse normal impact of a small mass. The Hertzian contact law was obtained from the elasto-plastic analysis of contact between a spherical impactor and an elastic rectangular. At this study, the focus is placed on the frictionless normal low velocity impact of a small sphere against an elastic mordantly thick rectangular plate (using Mindlin's plate theory). The natural frequencies and mode shapes of the plate are calculated by using the exact solution based on three coupled equilibrium equations. Finally, the influence of boundary conditions, dimensions of the plate, initial velocity and radius of the spherical impactor on the impact parameters are examined and discussed in detail.

Keywords: Impact, Rectangular Plate, Forced Vibration, Hertzian law;

1. Introduction

Impact of a sphere with a plate is a common phenomenon in engineering. Rectangular plates with different boundary conditions subjected to external loads have are the key components in aerospace, civil, automotive, biomechanical, petrochemical, marine industries, nuclear, optical, electronic, mechanical, and shipbuilding industries. They may also be rest on an elastic foundation.

Depending on the plate thickness, two main theories may be considered for modeling a rectangular plate. They are classical plate theory (CPT) and the first order shear deformation plate theory (FSPT). The CPT referred to Kirchhoff's theory (Leissa [1]), is only applicable for thin plates (due to ignoring the effect of shear deformation through the plate thickness and rotary inertia). In order to eliminate the deficiency of the classical plate theory for thick plates, the FSPT was proposed by Reissener [2] and Mindlin [3]. This theory is known as Mindlin plate theory. A usefull method for deriving the exact closed-

* Corresponding author. Tel.: +98-861-262-5700; fax: +98-861-262-5701.
E-mail address: k-khorshidi@araku.ac.ir.

1877-7058 © 2011 Published by Elsevier Ltd. Selection and peer-review under responsibility of ICM11
doi:10.1016/j.proeng.2011.04.290

form characteristic equation of vibrating moderately thick rectangular plates subjected to in-plane loading without elastic foundation (they combined boundary conditions, namely S-S-S-S, S-C-SS, S-C-S-C, S-S-S-F, S-F-S-F and S-C-S-F) was developed by Hosseini-Hashemi and Arsanjani [4] and Hosseini-Hashemi et al. [5]. Besides obtaining the response of the plate in free and forced vibrations, the impact event is deduced from the analytical solutions in literatures. Several researchers [6-12] have adopted the Hertzian's contact law in their studies. Troccaz et al. [13] developed a comprehensive model including calculations for both the impact force and the acoustic radiation. They studied the influence of the inelastic impact of a sphere on a simply supported rectangular plate. Sburlati [14] applied extension of the Levinson's displacement field in the dynamic case to find an exact solution for the impact law in thick elastic plates.

The aim of the research presented in this paper was to develop a more comprehensive model including calculations for both the forced vibration and the transverse elasto-plastic impact in the case of the impact of a small sphere on an elastic isotropic moderately thick rectangular plate with two parallel edges simply supported boundary conditions. The novelty of the paper is that the analytical closed-form solution is developed without any using approximation. The present analytical solution gives high accuracy and can be used as a benchmark. Meanwhile, the influence of boundary conditions, aspect ratios, thickness rations, foundation stiffness coefficients, in-plane loading factors, initial velocity and radius of the spherical impactor on the impact parameters are examined and discussed in detail.

2. Forced Vibration

Consider a flat, isotropic, rectangular Mindlin plate with uniform thickness of h, length a, width b, modulus of elasticity E, Poisson's ratio ν, and density per unit volume ρ, oriented so that its mid-plane surface contains the x_1 and x_2 axis of a Cartesian coordinate system (x_1, x_2, x_3). The plate was subjected to transverse normal impact of a small sphere mass. The combined boundary conditions of the plates are S-S-S-S, S-C-S-S, and S-C-S-C as shown in Fig. 1 [4, 5].

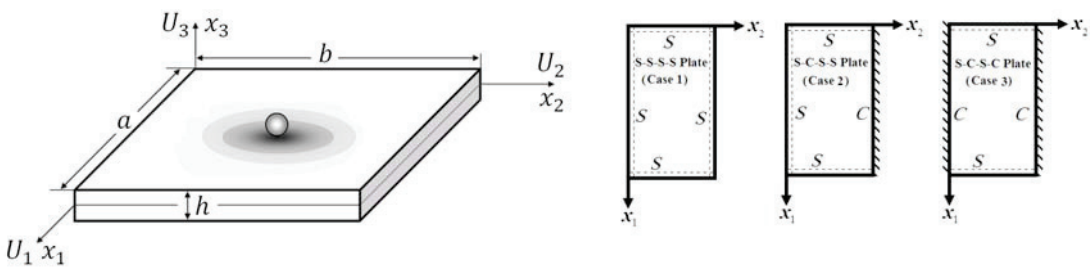

Fig. 1. A rectangular Mindlin plate with different boundary conditions subjected to impact of small mass

Consider the isotropic moderately thick rectangular plate subjected to dynamic transversely loading $\tilde{p}_3(X_1, X_2, \tilde{t})$. By the modal superposition method, the forced vibration of the plate is expressed as

$$\tilde{\chi}_1(X_1,X_2,\tilde{t}) = \sum_{m=1}^{\infty}\sum_{n=1}^{\infty}\tilde{\tilde{\psi}}_1^{mn}(X_1,X_2)T^{mn}(\tilde{t}),\ \tilde{\chi}_2(X_1,X_2,\tilde{t}) = \sum_{m=1}^{\infty}\sum_{n=1}^{\infty}\tilde{\tilde{\psi}}_2^{mn}(X_1,X_2)T^{mn}(\tilde{t}),$$
$$\tilde{\chi}_3(X_1,X_2,\tilde{t}) = \sum_{m=1}^{\infty}\sum_{n=1}^{\infty}\tilde{\tilde{\psi}}_3^{mn}(X_1,X_2)T^{mn}(\tilde{t}), \tag{1}$$

where $\tilde{\tilde{\psi}}_1^{mn}$, $\tilde{\tilde{\psi}}_2^{mn}$ and $\tilde{\tilde{\psi}}_3^{mn}$ are the modal shape functions and $T^{mn}(\tilde{t})$ is the principal coordinate for the (m,n) modal of the plate. Substituting Eqs. (1) into the governing differential equations for free vibration of the plate [4,5] gives

$$\sum_{m=1}^{\infty}\sum_{n=1}^{\infty}\left(\left[\tilde{\psi}_{1,11}^{mn}+\eta^2\tilde{\psi}_{1,22}^{mn}+\frac{\nu_2}{\nu_1}\overline{\left(\tilde{\psi}_{1,11}^{mn}+\eta\tilde{\psi}_{2,12}^{mn}\right)}-\frac{12\overline{\kappa^2}}{\delta^2}\overline{\left(\tilde{\psi}_1^{mn}-\tilde{\psi}_{3,1}^{mn}\right)}\right]T^{mn}(\tilde{t})\right)=\frac{\overline{\delta^2}}{12\nu_1}\sum_{m=1}^{\infty}\sum_{n=1}^{\infty}\left(\left[\tilde{\psi}_1^{mn}\right]\ddot{T}^{mn}(\tilde{t})\right),$$
$$\sum_{m=1}^{\infty}\sum_{n=1}^{\infty}\left(\left[\tilde{\psi}_{2,11}^{mn}+\eta^2\tilde{\psi}_{2,22}^{mn}+\frac{\nu_2}{\nu_1}\overline{\eta\left(\tilde{\psi}_{1,12}^{mn}+\eta\tilde{\psi}_{2,22}^{mn}\right)}-\frac{12\overline{\kappa^2}}{\delta^2}\overline{\left(\tilde{\psi}_2^{mn}-\eta\tilde{\psi}_{3,2}^{mn}\right)}\right]T^{mn}(\tilde{t})\right)=\frac{\overline{\delta^2}}{12\nu_1}\sum_{m=1}^{\infty}\sum_{n=1}^{\infty}\left(\left[\tilde{\psi}_2^{mn}\right]\ddot{T}^{mn}(\tilde{t})\right), \tag{2}$$

$$\sum_{m=1}^{\infty}\sum_{n=1}^{\infty}\left(\left[\tilde{\psi}_{3,11}^{mn}+\eta^2\tilde{\psi}_{3,22}^{mn}-\left(\tilde{\psi}_{1,1}^{mn}+\eta\tilde{\psi}_{2,2}^{mn}\right)\right]T^{mn}\left(\tilde{t}\right)\right)+\tilde{p}_3=\frac{\delta^2}{12\kappa^2\nu_1}\sum_{m=1}^{\infty}\sum_{n=1}^{\infty}\left(\left[\tilde{\psi}_3^{mn}\right]\ddot{T}^{mn}\left(\tilde{t}\right)\right),$$

where $\nu_1=\left(1-\nu\right)/2$, $\nu_2=\left(1+\nu\right)/2$, κ^2 is the shear correction factor, $\delta=h/a$ is the thickness ratio, $\eta=a/b$ is the aspect ratio and $\tilde{p}_3=p_3a/(12\kappa^2Gh)$. Using the governing differential equations for free vibration of the plate, the Eqs. (2a-c) will be obtained as

$$-\frac{\delta^2}{12\nu_1}\sum_{m=1}^{\infty}\sum_{n=1}^{\infty}\left(\left(\beta^{mn}\right)^2\left[\tilde{\psi}_1^{mn}\right]T^{mn}\left(\tilde{t}\right)\right)=\frac{\delta^2}{12\nu_1}\sum_{m=1}^{\infty}\sum_{n=1}^{\infty}\left(\left[\tilde{\psi}_1^{mn}\right]\ddot{T}^{mn}\left(\tilde{t}\right)\right),$$

$$-\frac{\delta^2}{12\nu_1}\sum_{m=1}^{\infty}\sum_{n=1}^{\infty}\left(\left(\beta^{mn}\right)^2\left[\tilde{\psi}_2^{mn}\right]T^{mn}\left(\tilde{t}\right)\right)=\frac{\delta^2}{12\nu_1}\sum_{m=1}^{\infty}\sum_{n=1}^{\infty}\left(\left[\tilde{\psi}_2^{mn}\right]\ddot{T}^{mn}\left(\tilde{t}\right)\right), \tag{3}$$

$$-\frac{\delta^2}{12\kappa^2\nu_1}\sum_{m=1}^{\infty}\sum_{n=1}^{\infty}\left(\left(\beta^{mn}\right)^2\left[\tilde{\psi}_3^{mn}\right]T^{mn}\left(\tilde{t}\right)\right)+\tilde{p}_3=\frac{\delta^2}{12\kappa^2\nu_1}\sum_{m=1}^{\infty}\sum_{n=1}^{\infty}\left(\left[\tilde{\psi}_3^{mn}\right]\ddot{T}^{mn}\left(\tilde{t}\right)\right).$$

Multiplying Eq. (3a) by $\nu_1\tilde{\psi}_1^{m'n'}$, Eq. (3b) by $\nu_1\tilde{\psi}_2^{m'n'}$, and Eq. (3c) by $\tilde{\psi}_3^{m'n'}12\kappa^2\nu_1/\delta^2$, respectively, and integration of the summation of these equations over the plate area gives

$$\ddot{T}^{mn}\left(\tilde{t}\right)+\left(\beta^{mn}\right)^2T^{mn}\left(\tilde{t}\right)=\frac{Q^{mn}\left(\tilde{t}\right)}{K^{mn}}, \tag{4}$$

where

$$K^{mn}=\int_0^1\int_0^1\left(\frac{\delta^2}{12}\left(\left(\tilde{\psi}_1^{mn}\right)^2+\left(\tilde{\psi}_2^{mn}\right)^2\right)+\left(\tilde{\psi}_3^{mn}\right)^2\right)dX_1dX_2\ ,\ Q^{mn}\left(\tilde{t}\right)=\int_0^1\int_0^1\left(\tilde{F}\left(\tilde{t}\right)g\left(X_1,X_2\right)\tilde{\psi}_3^{mn}\right)dX_1dX_2 \tag{5}$$

and $\tilde{F}\left(\tilde{t}\right)g\left(X_1,X_2\right)=(12k^2\nu_1/\delta^2)\tilde{p}_3$. Zero initial conditions are assumed, i.e.,

$$\left(\tilde{\psi}_1^{mn},\tilde{\psi}_2^{mn},\tilde{\psi}_3^{mn}\right)_{\tilde{t}=0}=0\quad,\quad\left(\frac{\partial\tilde{\psi}_1^{mn}}{\partial\tilde{t}},\frac{\partial\tilde{\psi}_2^{mn}}{\partial\tilde{t}},\frac{\partial\tilde{\psi}_3^{mn}}{\partial\tilde{t}}\right)_{\tilde{t}=0}=0, \tag{6}$$

the Eq. (4), then is written in form of Eq. (8)

$$T^{mn}\left(\tilde{t}\right)=\frac{1}{K^{mn}\beta^{mn}}\int_0^{\tilde{t}}Q^{mn}\left(\tau\right)\sin\beta^{mn}\left(\tilde{t}-\tau\right)d\tau\ . \tag{8}$$

Substituting the Eq. (8) into e Eq. (1), $\tilde{\chi}_1\left(X_1,X_2,\tilde{t}\right)$, $\tilde{\chi}_2\left(X_1,X_2,\tilde{t}\right)$, and $\tilde{\chi}_3\left(X_1,X_2,\tilde{t}\right)$ will be obtained. The force vibration response of a plate (the transverse deflection) under transverse point force subjected at (X_1^*,X_2^*) is represented as

$$\tilde{\chi}_3\left(X_1,X_2,\tilde{t}\right)=\sum_{m=1}^{\infty}\sum_{n=1}^{\infty}\frac{\tilde{\psi}_3^{mn}\left(X_1,X_2\right)\tilde{\psi}_3^{mn}\left(X_1^*,X_2^*\right)}{K^{mn}\beta^{mn}}\int_0^{\tilde{t}}\tilde{F}\left(\tau\right)\sin\beta^{mn}\left(\tilde{t}-\tau\right)d\tau \tag{9}$$

3. *Elasto-plastic Impact law in moderately thick rectangular plates[6]*

In this paper the elasto–plastic contact law for permanent deformation and unloading was employed to analyze the small mass impact response of elastic rectangular plates. In this law, the contact can be divided into the three phases. The first phase is assumed to be elastic indentation Hertzian behavior. In the second phase, the elastic–plastic indentation is initiated a plastic where the yielding" point is exceeded. Restitution in third phase is initiated when the relative velocity is zero. The quasi-static contact law for the three phases is given as following:

Phase I: Elastic indentation

In Hertz contact theory, the impact force of a sphere on the elastic rectangular plate and in the original co-ordinate is given by

$$\left(\frac{F(t)}{k_2}\right)^{2/3}=V_bt-\frac{1}{m_b}\int_0^t(t-\tau)F(\tau)d\tau-\psi_3(x_1^*,x_2^*,t) \tag{10}$$

where $\psi_3(x_1^*, x_2^*, t)$ is the transverse response at the point of impact load, $F(t)$ is the contact force, $m_b = (4/3)\rho_b \pi R^3$, ρ_b, R and V_b are the mass, density, radius, and initial velocity of the impactor, respectively. k_2 is the contact stiffness and can be expressed as

$$k_2 = \frac{4\sqrt{R}}{3\pi(\delta_p + \delta_b)}, \ \delta_p = \frac{1-\nu^2}{\pi E}, \ \delta_b = \frac{1-\nu_b^2}{\pi E_b}, \tag{11,12}$$

where E_b and ν_b are the modulus of elasticity and Poisson's ratio of the impactor, respectively. The relationship between the contact force and indentation (difference between the displacement of the impactor and the plate) can be described as

$$\alpha(t) = \left(\frac{F(t)}{k_2}\right)^{2/3} \tag{13}$$

The contact radius a, the contact stress distribution within contact radius q, and contact velocity V are written as Eqs. (14)

$$a = \sqrt{R\alpha}, \quad q = \frac{q_0}{a}\sqrt{a^2 - r^2}, \quad V = \frac{d\alpha}{dt}, \ q_0 = \frac{3F}{2a^2\pi} \tag{14}$$

where $0 \le r \le a$ and q_0 is the maximum normal stress in the contact zone.

Phase II: Elasto-Plastic indentation

The second phase is started when the maximum normal stress is more than dynamic yielding stress i.e. $q_0 \ge q_c$. For the elasto-plastic loading phase, the governing equation is

$$\frac{F(t)}{\pi R q_c} + \frac{\alpha_1}{3} = V_b t - \frac{1}{m_b}\int_0^t (t-\tau)F(\tau)d\tau - \psi_3(x_1^*, x_2^*, t) \tag{15}$$

where α_1 is the critical indentation when the plastic deformation starts, it is expressed as Eq. (16)

$$\alpha_1 = \frac{R\pi^2 q_c^2 \left(1-\nu^2\right)^2}{4E^2} \tag{16}$$

and indentation and radius of plastic zone in second phase can be described as

$$\alpha(t) = \frac{F(t)}{\pi R q_c} + \frac{\alpha_1}{3}, \quad r_p = \sqrt{R\left(\alpha(t) - \alpha_1\right)}. \tag{17}$$

At the end of elasto-plastic phase, the velocity between the impactor and the plate becomes zero. After that, the unloading or restitution accures.

Phase III: Elastic restitution

For the elasto-plastic loading phase the governing equation is

$$F(t) = \frac{2}{\pi R\left(\delta_p + \delta_b\right)}\left(r_p^2\left(R\alpha(t) - r_p^2\right)^{1/2} + \frac{2}{3}\left(R\alpha(t) - r_p^2\right)^{3/2}\right)q_c, \tag{18}$$

and

$$\alpha(t) = V_b t - \frac{1}{m_b}\int_0^t (t-\tau)F(\tau)d\tau - \psi_3(x_1^*, x_2^*, t), \tag{19}$$

In this paper, a Mathematia (version 7) program was employed. The Eqs. (10), (15), and (18) were solved using small time increment method (STIM).

4. *Results and discussion*

After finding the analytical solution of the present problem, the following results for the elasto-plastic impact response of isotropic r moderately thick rectangular plates with two opposite edges are simply supported and any of the other two edges can be simply supported or clamped for various geometrics (i.e. aspect ratios and thickness to length ratios) are discussed in this section. The results presented in this section are for the impact between a 7.8-mm-diameter steel sphere (the material properties of the impactor are; $\nu_b = 0.3$, $\rho_b = 7800\,kg/m^3$ and $E_b = 200\,GPa$) and a 405×325×3-mm Aluminium plate (the material properties of the plate are; $\nu = 0.34$, $\rho = 2700\,kg/m^3$, $E = 70\,GPa$ and $q_c = 324.018\ MPa$). It should be noted that the shear correction factor of $\kappa^2 = 0.86667$ was used.

4.1. Effect of impactor radius on the impact parameters

Fig. 2 shows the effect of impact radius on the contact force and indentation history of a simply supported Aluminum square Mindlin plates with $\delta = 0.1$ and $a = 1m$. This plate is impacted by steel sphere with $V_b = 1m/s$. It can be easily observed that, as the radius of impactor increases from 0.02 m to 0.04 m, the contact force and indentation history increase. The duration of the contact force and indentation history also increases with the increase of the impactor radius.

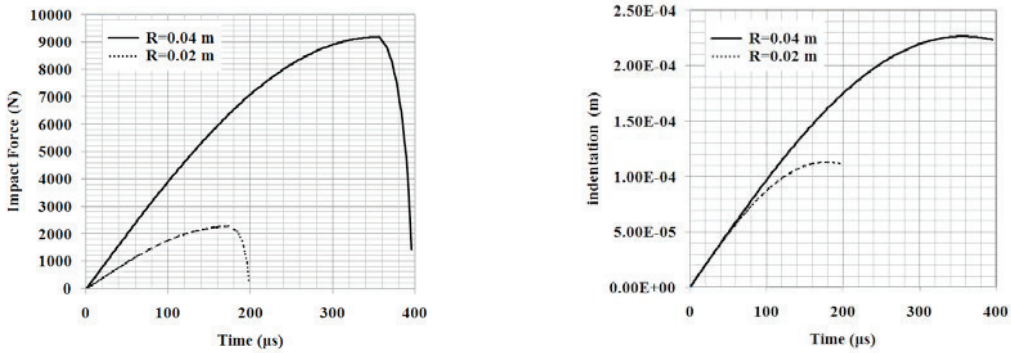

Fig. 2. Contact force and indentation history of a simply supported Aluminum square Mindlin plates impacted by steel sphere with various radiuses.

4.2. Effect of impactor velocity on the impact parameters

The effect of the initial velocity of the impactor with $R = 0.04m$ on the impact parameters of the S-C-S-C Aluminum plate with $\eta = 1$, $\delta = 0.1$ and $a = 1m$ was also investigate displayed in Fig. 3. For the same plate and size of impactor the maximum initial velocity of impactors, the greater contact forceand indentation history furthermore, the duration of the contact force and indentation history decreases with the increase of the impactor velocity.

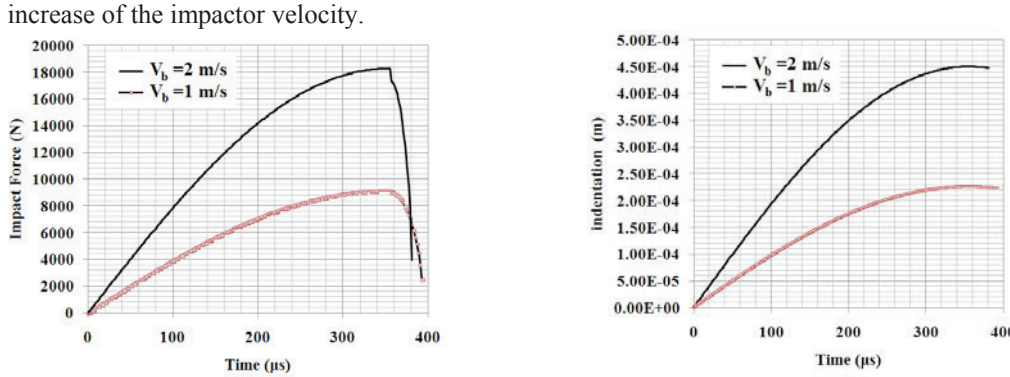

Fig. 3. Contact force and indentation history of a S-C-S-C boundary conditions Aluminum square Mindlin plates impacted by steel sphere with various initial velocities.

4.4. Effect of aspect ratio on the impact parameters

In order to study the effect of the aspect ratio on the contact force and indentation history, Fig. 4 was plotted. The results shown in Fig. 4 were obtained for the Aluminum simply supported plate with $\delta = 0.1$ and $a = 1m$ which is impacted by a steel sphere with $V_b = 1m/s$ and $R = 0.04m$. It is observed that, the contact force decrease with increasing the plate aspect ratio η while the thickness ratio δ and radius and velocity of impactor are constant and the indentation remains the same. This observation indicates that, between two plates with the same length *a*, thickness *h* and boundary conditions, the narrow plate reaches to smaller contact force.

4.7. Effect of boundary conditions on the impact parameters

The influences of the different boundary conditions on the imapact parameters are presented in Table 1 for constant dimensions and material properties of the plate and impactor. The results presented in Table 1, show that the lowest critical contact force and indentation history correspond to the plates with more constraints. As the number of supported edges increases, the contact force and indentation history also increase. Among all the three boundary conditions, it can be seen that the lowest and highest values of contact force and indentation history correspond to S-C-S-C and S-S-S-S cases, respectively.

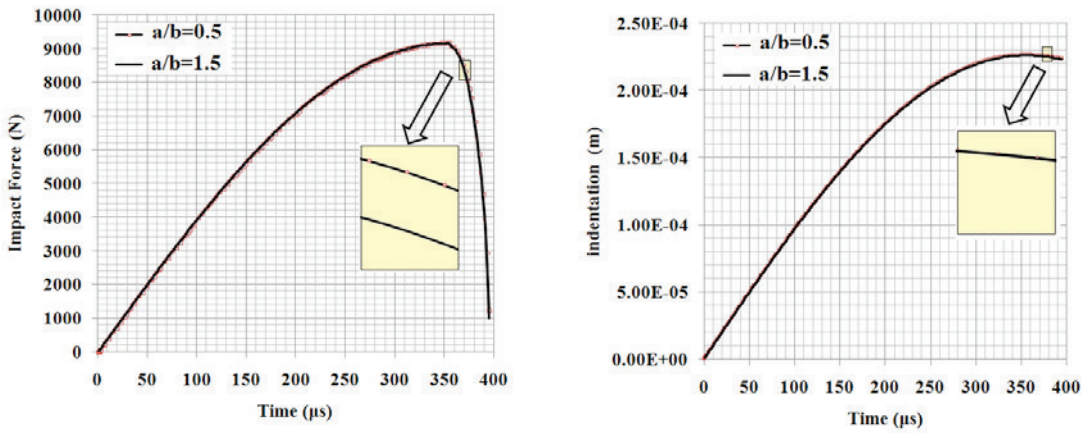

Fig. 4. Contact force and indentation history of a simply supported Aluminum square Mindlin plates with various aspect ratios impacted by steel sphere.

Table 1. Variation of impact parameters, for different boundary conditions of Aluminum square Mindlin plates ($\delta = 0.1$, $a = 1m$) under impact of steel sphere ($V_b = 1m/s$, $R = 0.04m$).

Impact Parameters	Boundary Conditions	Phase I	Phase II	Phase III
$t(\mu s)$	S-S-S-S	3	355	395
	S-C-S-S	3	355	395
	S-C-S-C	2	358	414
$\alpha(\mu s)$	S-S-S-S	2.9999	266.153	223.184
	S-C-S-S	2.9999	266.153	223.183
	S-C-S-C	1.9997	219.186	217.189
$F(N)$	S-S-S-S	80.6309	9167.63	0
	S-C-S-S	80.6309	9167.61	0
	S-C-S-C	44.3700	8897.54	0

5. Refrences

[1] Leissa, A.W., Vibration of Plates. NASASP-169, Office of Technology Utilization, NASA, Washington, DC; 1969. Reprinted by The Acoustical Society of America; 1993.

[2] Reissner, E. The effect of transverse shear deformation on the bending of elastic plates. Trans. ASME J. of Applied Mechanics 1945; 12: 69-77.

[3] Mindlin, R.D. Influence of rotary inertia and shear in flexural motion of isotropic elastic plates. Trans. ASME J. of Applied Mechanics 1951; 18:31-38.

[4] Hosseini-Hashemi, Sh. and Arsanjani, M. Exact Characteristic Equations for Some of Classical Boundary Conditions of Vibrating Moderately Thick Rectangular Plates. Int. J. of Solids and Structures 2005; 42: 819-853.

[5] Hosseini-Hashemi, Sh., Khorshidi, K. and Amabili, M. Exact solution for linear buckling of rectangular Mindlin plates. J. of Sound and Vibration 2008; 315 (1-2): 318-342.

[12] Jones, N. Structural impact. Cambridge: Cambridge University Press; 1989.

[13] Koller, M.G. and Busenhart, M. Elastic impact of spheres on thin shallow spherical shells. Int. J. of Impact Engineering 1986; 4: 11–21.

[14] Mittal, R.K. A simplified analysis of the effect of transverse shear on the response of elastic plates to impact loading. Int. J. of Solids and Structures 1987; 23 (8): 1191–1203.

[15] Chattopadhyay, S. Permanent indentation effects on the impact response of elastic plates. J. Acoustical Society of America 1987; 82: 493–497.

[16] Lee, D.I. and Kwak, B.M. An analysis of low-velocity impact of spheres on elastic curved-shell structures. Int. J. of Solids and Structures 1993; 30: 2879–2893.

[17] Liu Z.S. and Swaddiwudhipong, S. Response of plate and shell structures due to low velocity impact. ASCE J. Engineering Mechanic 1997; 123 (12): 1230–1237.

[18] Liu, Z.S., Lee, H.P. and Lu, C. Structural intensity study of plates under low-velocity impact. Int. J. of Impact Engineering 2005; 31 (8): 957-975.

[19] Troccaz, P., Woodcock, R. and Lavillec, F. Acoustic radiation due to the inelastic impact of a sphere on a rectangular plate. J. Acoustical Society of America 2000; 108 (5): 2197-2202.

[20] Sburlati, R. An exact solution for the impact law in thick elastic plates. Int. J. of Solids and Structures 2004; 41: 2539–2550.